Fundamental Journal of Mathematical Physics
Vol. 4, Issues 1-2, 2015, Pages 1-21
Published online at http://www.frdint.com/

PARTIAL FILLED TANK EFFECT WITHOUT BULKHEAD AND WITH ONE BULKHEAD ON SHIP STABILITY USING VOLUME-OF-FLUID METHOD

N. COULIBALY[a,*], LASSANA SAMASSI[b] and M. DOSSO[b]

[a]Laboratoire de Mécanique et Energétique
UFR Mathématiques et Informatique
Université Félix Houphouêt Boigny Abidjan-Cocody
22 BP 582 Abidjan 22
Ivory Coast
e-mail: coulnamson@hotmail.com

[b]Laboratoire de Mathématiques Appliquées
UFR Mathématiques et Informatique
Université Félix Houphouêt Boigny Abidjan Cocody
Ivory Coast
e-mail: mouhamadou.dosso@univ-fhb.edu.ci

Abstract

Ship Stability depends on the position of gravity of the ship relative to the metacentre essentially. However, when there is a partially filled tank on board, stability criterion becomes severe, that is the ship may be unstable, which could cause the capsizing. In this paper, implicit finite volume method and an algebraic volume of fluid method will be used to study the effect of a partial filled tank onboard on ship stability. Numerical results of sloshing in a partially filled rectangular tank with one bulkhead will be presented here.

Keywords and phrases: metacentric height, stability, finite volume method, volume-of-fluid, free surface, two-phase flow, resonance.

2010 Mathematics Subject Classification: 65M08, 65N08, 74S10.

*Corresponding author

Received December 26, 2014

1. Introduction

The ship safety issues are crucial from the operational point of view and they can be considered as one of the most prospective technical affairs. One of the most critical features of seagoing ship related to her safety is the transverse stability. Ship stability is defined as the tendency of a ship to return back to her equilibrium when she is inclined from an upright position. This means that the metacentre M is above the centre of gravity G, that is the metacentric height $\overline{GM}$ is positive. In the case, this value is negative, in other words the metacentre M is under G, the ship is said to be unstable [1, 2, 3].

Free surface can be modelling using two approaches: interface tracking approach and interface capturing approach. In the first one approach, the free surface is located at one boundary of the mesh, and the mesh deforms as the free surface moves [18, 19, 20]. It is an explicit representative approach of the surface. They define the free surface as a sharp interface whose motion is followed. The tracking is usually performed by making use of the kinematic and dynamic free surface boundary conditions. The second approach is characterized by an implicit representation of the interface which is tracked as part of the solution algorithm. The computations are performed on a fixed grid, which extends beyond the free surface. These methods are also called volume tracking methods [21, 22, 23, 24]. They have a wide range of applications including problems in fluid mechanics, combustion, manufacturing of computer chips, computer animation, image processing Structure of snowflakes, the shape of soap bubbles, satellite controllability.

In this paper, an algebraic volume-of-fluid method referred to Compressive Interface Capturing Scheme for Arbitrary Mesh (CICSAM) is used. However, pioneering work of VOF methods goes back to the early 1970s: DeBar [23] in 1974, Noh and Woodward [24] in 1976, Ramshaw and Trapp [25] in 1976 and Peskin [26] in 1977, but with Hirt and Nichols [27] in 1981 and their SOLA-VOF code, the method became widely used.

For a given velocity field (provided by a flow solver), interfaces (free surface) are then tracked by evolving fluid volumes in time with the solution of an advection equation. Volume fraction results from normalization of fluid volume relative to the cell volume. At any time in the solution, an exact interface location is not known, i.e., a given distribution of volume fraction data does not guarantee a unique interface topology. Interface geometry is instead inferred (based on assumptions of the particular algorithm) and its location is then reconstructed from local volume fraction data. Typically, one can reconstruct the interface by the straightforward SLIC (Simple Line Interface Calculation) methods as in [24, 38] and [39] or by various PLIC (Piecewise Linear Interface Calculation) methods [28, 29, 30, 31] and [32]. The latter methods give much better results than the former, as noted in the review achieved by Kothe and Rider [33]. However, a major drawback of geometric approach described above, is that, the cell shapes are implicitly used in the interface reconstruction and so it is difficult to extend these techniques to arbitrary complex three dimensions curvilinear coordinates system. In [34], a Cartesian geometric approach is achieved by introducing aperture approach (cut cell approach) which indicates the fraction of the cell and cell face that is open for the flow. Another drawback of geometric approach is the estimation of the interface normal, which influences the interface shape.

Alternatively, an algebraic approach can be adopted in which the convective scalar transport equation for volume fraction is discretised in such as way to guarantee physical (bounded) volume fraction whilst preventing smearing of the interface over several mesh cells as in [35, 36 and 37].

2. Numerical Formulation

2.1. Free surface effect

The free surface motion of the liquid in a tank reduces a ship's stability because, as the ship is inclined, the centre of gravity of the liquid in the tank shifts toward the low side. This causes the ship's centre of gravity to move toward the low side, reducing the righting arm $\overline{GZ}$ which depends on the metacentric height as

$$GZ = GM \sin \theta. \tag{1}$$

The metacentric height is given by

$$\overline{GM} = \overline{KB} + \overline{BM} - \overline{KG}, \tag{2}$$

where the metacentric radius is given by Bouger formulae

$$\overline{BM} = \frac{I}{\nabla}, \tag{3}$$

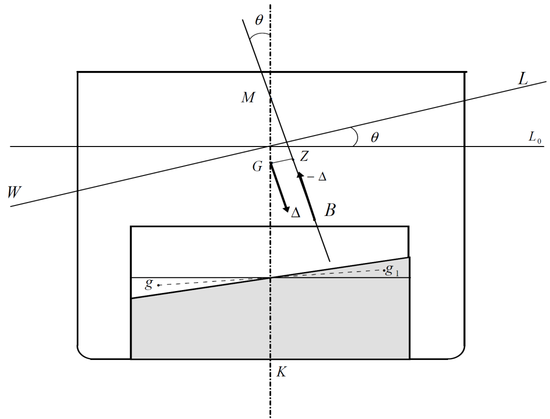

Figure 1. Free surface effect on ship stability.

where I is the moment of inertia of area of waterplane of the ship about the axis of heeling and ∇ is the displacement of the ship, that is, the volume of the immersed part of the ship.

Now let the ship be floating right initially at a waterline $W_0 L_0$ and let it be heeled through a small angle θ to a new waterline WL. The free surface in the partially filled tank will be inclined by the same angle θ as shown in Figure 2.1. As a result to the heel, some of the liquid in tank will flow from the high side to the low side of the tank and a heeling moment will exist equal to product of the weight of the shifted liquid by the distance gg_1, since the center of gravity of the wedge shifts from g to g_1. It is well known that when partly filled tank is on board, the metacentric height of a ship becomes [4, 5, 6]

$$\overline{GM} = \overline{KB} + \overline{BM} - \overline{KG} - \frac{\rho_L I_{Fs}}{\rho \nabla}, \tag{4}$$

where I_{Fs} is the moment of inertia of the free surface area inside the tank about a longitudinal axis through the centroid of that area, ρ_L is the density of liquid inside the tank, ρ is the density of water in which the ship is floating. The last term in (4) is the effect of the free surface on ship stability and it is called the *virtual loss* of $\overline{GM}$. Any loss in $\overline{GM}$ is a loss in stability. For example, if free surface be created in a ship with a small initial metacentric height, the virtual loss of $\overline{GM}$ due to free surface may result in a negative metacentric height. This could cause the ship to take up an angle of loll which may be dangerous in any case is undesirable.

Free surface effect on ship stability may be reduced by subdivision of the tank using some bulkhead, since the moment of inertia depends on the aera of the free surface. It is well known that by subdividing the tank into $n+1$ compartments, the moment of inertia is then divided by $(n+1)^2$, as in [3, 4, 5, 6].

$$\overline{GM} = \overline{KB} + \overline{BM} - \overline{KG} - \frac{\rho_L I_{Fs}}{(n+1)^2 \rho \nabla}, \tag{5}$$

where n is the number of bulkheads.

From relation (5), it is obvious that when the number of bulkheads becomes large, the last term tends toward zero. So the effect of free surface on ship stability may be reduced by tank subdivision using bulkheads. In this paper, we have studied the free surfaces of two partly filled tank problems. The first one concerns a rectangular tank without any bulkhead. The second study is devoted to the same tank subdivided by one bulkhead. Here, the tank is subjected to harmonic horizontal oscillations as in [10, 11].

2.2. Governing equations

The motion of the incompressible two-phase flow inside the tank is described by the Navier Stokes equations:

- Continuity equation

$$\frac{\partial u_i}{\partial x_i} = 0. \tag{6}$$

- Momentum equations

In this first test, a rectangular tank with fluid inside is initially at rest state [14]. An experimental test was performed in [12, 7 and 8]. The tank is suddenly accelerated along the horizontal *x*-direction in a sinusoidal large-amplitude. The position of the tank is given by

$$x = A \sin \frac{2\pi}{T} t \quad \text{and} \quad y = cte. \tag{7}$$

The inertial body force due to oscillations is given by

$$F_i = -\rho V \ddot{x}, \tag{8}$$

where V is the volume of the liquid inside the control volume, and $\ddot{x}$ is the acceleration of the governing coordinate system which is given by

$$\ddot{x} = -A\omega^2 \sin \frac{2\pi}{T} t. \tag{9}$$

The momentum equations become

$$\frac{\partial u_i}{\partial t} + \frac{\partial u_i u_j}{\partial x_j} = -\frac{1}{\rho}\frac{\partial p}{\partial x_i} + \frac{\partial}{\partial x_j}\left(\nu\left(\frac{\partial u_i}{\partial x_j} + \frac{\partial u_j}{\partial x_i}\right)\right) + g_i + \frac{f_i}{\rho} - \rho\ddot{x}_i \tag{10}$$

with

$$\rho = \rho_l + (1 - F)\rho_g \quad and \quad \nu = \nu_l + (1 - F)\nu_g. \tag{11}$$

In the above equations, u_i and g_i are the Cartesian velocity and the gravity components in i-direction, respectively; p is the pressure; μ_k and ρ_k are the viscosity and density respectively of the fluid k, where $k = g$ for gas and $k = l$ for liquid. The last term f_i is the surface tension force obtained via the continuum surface force CSF approach [13, 14], which is active only on liquid-gas interface.

- Volume fraction equation

The properties (density and viscosity coefficients) appearing in the momentum equation are determined by the presence of the component phase (volume fraction) F in each control volume, which is bounded by zero and one. It could be defined as the filling degree of each cell. When the cell is full of liquid (water) the volume fraction $F = 1$, then if the cell is full of air (gas) $F = 0$, and when the cell contains the free surface, that is gas and liquid, then $0 < F < 1$.

$$\frac{\partial F}{\partial t} + \frac{\partial F u_i}{\partial x_i} = 0. \tag{12}$$

2.3. Discretization of governing equations

- Momentum equations

The purpose of any discretization practice is to transform one or more partial differential equations into a corresponding system of algebraic equation as is detailed in [15, 16, 17]. The finite volume discretization of ui-momentum equation is based on the integration over the control volume and time step. Quadratic Upwind Interpolation of Convective Kinetics (QUICK) scheme of Hayase et al. [40] is used for convective terms and central difference for diffusive terms and fully implicit time scheme. In order to avoid the numerical instability, often known as the “checkerboard problem, an improved Rhie-Chow interpolation [41] is used to calculate the convective. The spatial and temporal discretization leads to the form of linear matrix equations as

$$Ax = b, \tag{13}$$

where

- A is the matrix obtained from discretisation of momentum,

- b is the vector which includes volume forces, extra terms of convective terms of high order such as in TVD scheme [42] and scheme of Hayase [40],

- x is the unknown nodal velocity vector.

- Free surface equation

The crucial issue for modeling of the multiphase flow is a proper solution of equation (12), i.e., the discretization of time derivative and nonlinear convective term. A desirable property of an advection scheme is that it should be “monotonicity preserving” or “shape-preserving”; that is, it should not create spurious extrema or cause spurious amplification of existing extrema in an advected quantity. Standard advection techniques can not guarantee this desirable property since, these schemes are usually too diffusive and cannot guarantee the sharpness of the multi-fluid interfaces essential in free surface problems on stationary meshes. This desirable property can be achieved by carefully constraining or “limiting” the advective fluxes calculated by the scheme. This can be achieved by use of High Resolution Schemes like Total Variation Diminishing (TVD) scheme [42, 43, 44, 45] and Normalized Variables Diagrams (NVD) [46, 47, 48, 49] and [50]. In this paper, the CICSAM scheme is used to calculate the advective flux.

Integration of equation (12) over the control volume gives to

$$\frac{F_P^{n+1} - F_P^n}{\Delta t} + F_e u_e S_e - F_w u_w S_w + F_n u_n S_n - F_s u_s S_s = 0, \tag{14}$$

where F_P^n indicates the value of the volume fraction at central node P of the control volume at time step n; u_f is the velocity at cell face f; i.e., east, west, north and south; S_f is the area of the cell face f; and F_f is the value of the volume fraction at cell face f which can produce numerical diffusion of the free surface if it is not properly calculated, see Figure 2.

Normalized Variable Diagram provides the foundation for CICSAM scheme. It is based on the convective boundedness criterion that states that the variable distribution between the centers of neighborhood control volumes, e.g., D and A should remain smooth $F_D \leq F_f \leq F_A$, see Figure 3.

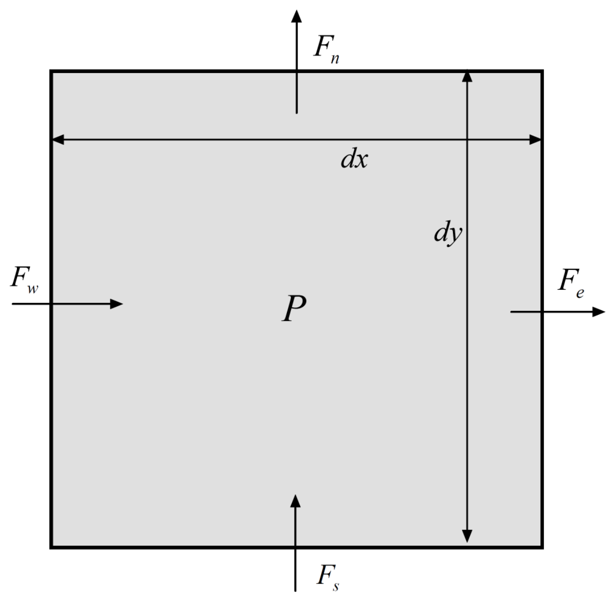

Figure 2. Control volume with node P.

Using this constraint about value of the variable in the upwind control volume F_U, normalized variables are defined as

$$\tilde{F}_f = \frac{F_f - F_U}{F_A - F_U}, \tag{15}$$

$$\tilde{F}_D = \frac{F_D - F_U}{F_A - F_U}. \tag{16}$$

The boundedness criterion can be rewritten using equations (15) and (16) as $\tilde{F}_D \leq \tilde{F}_f \leq 1,$ what can be shown through a diagram where the boundedness criterion is satisfied by any differential scheme.

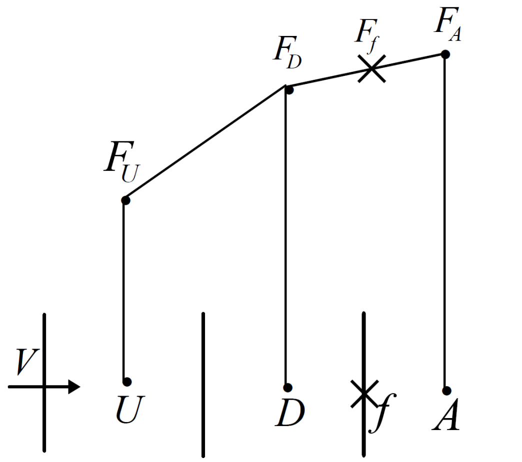

Figure 3. Boundedness criterion, *U* upwind, *D* donor and *A* acceptor cells.

In the case of the CICSAM scheme, additional assumption about the dependence of the region where the CBC is satisfied on the CFL condition, is used as in [51] by

$$\tilde{F}_D \leq \tilde{F}_f \leq \min\left(1, \frac{\tilde{F}_D}{C_f}\right), \tag{17}$$

where the local value of the Courant number defined at the face *f* of the control volume is

$$C_f = u_f S_f \frac{\Delta t}{V_P}, \tag{18}$$

where V_P is the volume of the cell *P*.

One needs to notice, that for explicit schemes, if the local value of the Courant number C_f tends towards unity, only the UD scheme satisfies the CBC criterion $\tilde{F}_f \to \tilde{F}_D,$ see Figure 4.

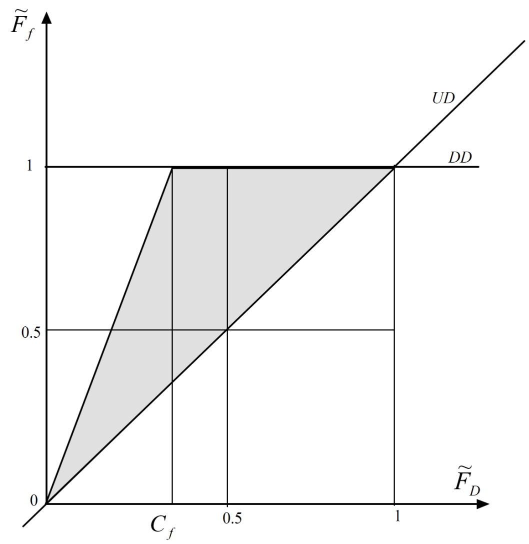

Figure 4. Dependance of the CBC region on local CFL condition.

The CICSAM scheme combines two high order schemes. The first one that is shown to be compressive, is known as the *HYPER-C scheme*

$$\tilde{F}_{fCBC} = \begin{cases} \tilde{F}_f = \tilde{F}_D & : \quad 0 < \tilde{F}_D,\ \tilde{F}_D > 1, \\ \min\left(1,\ \dfrac{\tilde{F}_D}{C_f}\right) & : \quad 0 \le \tilde{F}_D \le 1. \end{cases} \tag{19}$$

However, compressive character of the *HYPER-C* is not always desirable. It means that it changes any gradient to a step profile due to the downwind differencing scheme employed. When interface is tangential to the flow direction it is shown that aforementioned scheme tends to artificially deform its shape. For this reason it is found to be necessary to switch between *HYPER-C* scheme and other less compressive formulation such as the ULTIMATE-QUICKEST scheme which is the order accurate QUICK:

$$\tilde{F}_{fUQ} = \begin{cases} \tilde{F}_f = \tilde{F}_D & : \quad 0 < \tilde{F}_D,\ \tilde{F}_D > 1 \\ \min\left(\tilde{F}_{fCBC},\ \dfrac{8C_f\tilde{F}_D + (1 - C_f)(6\tilde{F}_D + 3)}{8}\right) & : \quad 0 \le \tilde{F}_D \le 1 \end{cases}. \tag{20}$$

A linear blending is used to switch smoothly between both schemes with a blending factor α_f. Now for CICSAM scheme, the value of the volume fraction $\tilde{F}_f$ is given by

$$\tilde{F}_f = \alpha_f \tilde{F}_{fCBC} + (1 - \alpha_f)\tilde{F}_{fUQ}, \tag{21}$$

where

$$\alpha_f = \min\left(1, \frac{1 + \cos 2\theta_f}{2}\right), \tag{22}$$

where

$$\theta_f = \arccos\left|\vec{d}.\vec{n}\right|, \tag{23}$$

where the unit vector parallel to the line between the donor cell *D* and acceptor cell *A* is

$$\vec{d} = \frac{\overrightarrow{DA}}{DA} \tag{24}$$

and the unit vector normal to the interface in donor cell *D* is

$$\vec{n} = \frac{\nabla F_D}{|\nabla F_D|}. \tag{25}$$

To extend the CICSAM scheme to *n*-dimension flow, cell Courant number C_D is introduced as

$$C_D = \sum_{f=1}^{n} \max(C_f, 0). \tag{26}$$

3. Numerical Results and Discussions

3.1. Model setup

We consider a partially filled rectangular tank in horizontal oscillations as it was mentioned in Subsection 2.2. The dimensions of the tanks are as follow length and height $1.0\,\text{m}$ and $0.5\,\text{m}$, respectively. The fluid properties, namely the viscosity and the density are $\mu = 10^{-3}\,\text{kg.m}^{-1}.\text{s}^{-1}$ and $\rho = 10^{3}\,\text{kg.m}^{-3}$. The filling ratio of the tank is 53%, that is, the initial height of water inside the tank $0.265\,\text{m}$. The computational mesh consists of 201×101 cells or control volumes. The period and the magnitude of the tank oscillation are $T = 2\text{s}$ and $A = 0.2\text{ m}$, respectively. Two tests are studied in this paper as follows.

3.2. Tank without bulkhead

Following figures show the snapshots of our simulations. It is noticed that the amplitude of sloshing of water inside the tank increases until we can observe the impact of the wave on the floor. This phenomena is known as the resonance as it is shown in [36] and [37].

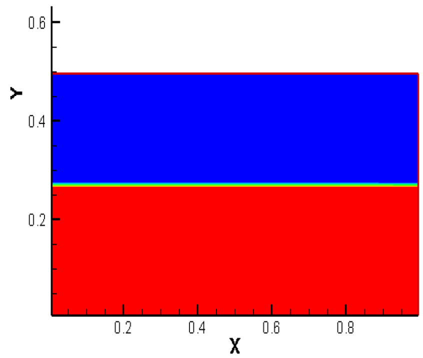

$T = 0\text{ s}$.

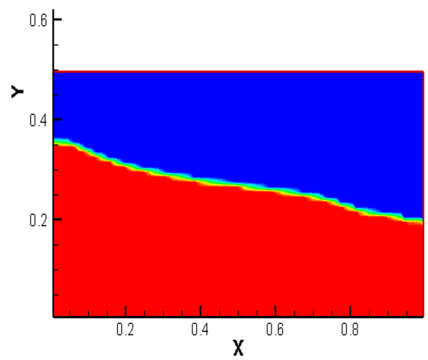

$T = 0.3\text{ s}$.

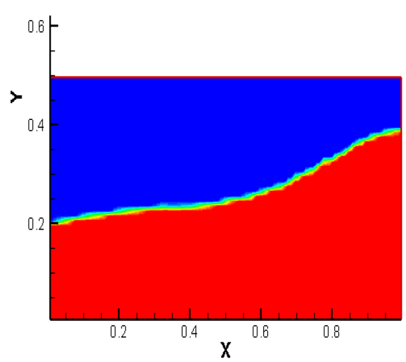

$T = 0.9\text{ s}$.

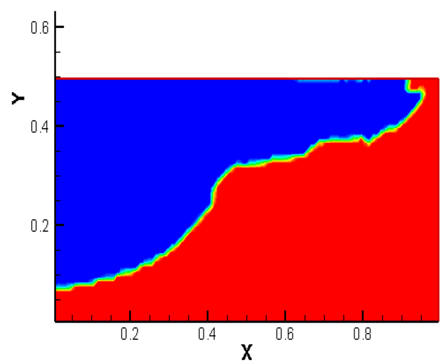

$T = 0.5\text{ s}$.

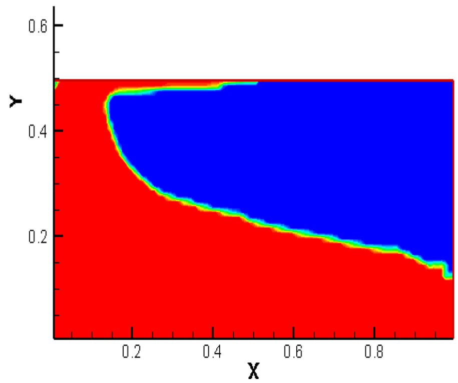

$T = 0.5\,\text{s}.$

Figure 5. Sloshing in tank without bulkheads.

The following curves show the heights of liquid at probes 1 and 2 located on left and right wall of the tank on initial free surface. In other words probe 1 is at $(x = 1,\ y = 0.265)$ and probe 2 is at $(x = i\max,\ y = 0.265)$. We can notice that some peaks are constant that is due when the liquid is in contact with the floor of the tank as it is illustrated above. The period of sloshing from simulation results is almost equal to the period of excitation of the tank which confirms the resonance.

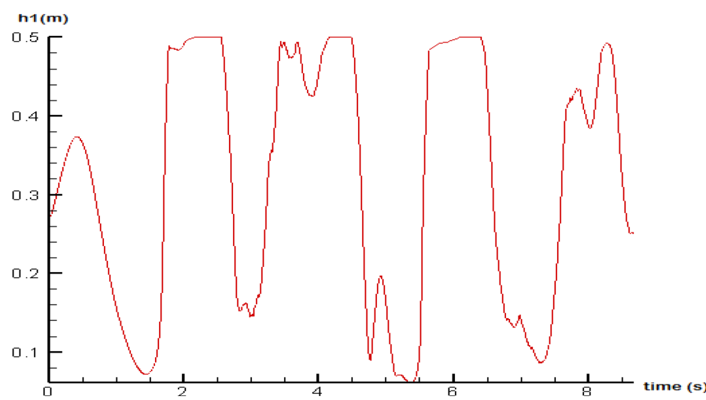

(a)

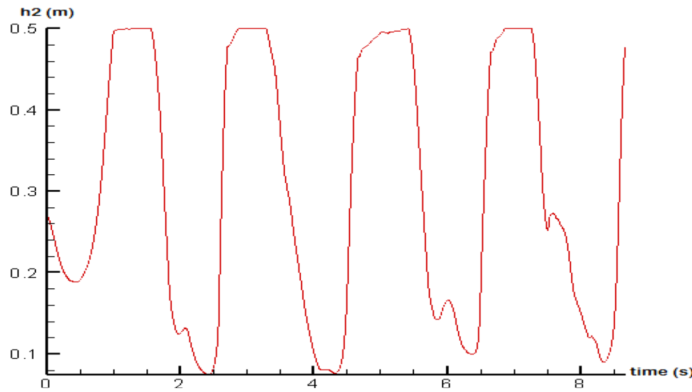

(b)

Figure 6. Heights of water at probes 1 and 2.

The pressure (in Pascal) at points $A\ (x = 0.5,\ y = 0.05)$ and $B\ (x = 1,\ y = 0.265)$ are shown in Figure 7 .The period of pressure oscillations is near $T = 2\,\text{s}$. Point A is bottom, the pressure is more large because of additional hydrostatic pressure. Point B is on initial free surface where atmospheric pressure is assumed to null. Hence when the point B is in air region the pressure becomes zero and when it is in water the pressure increases until $1000\,\text{Pa}$.

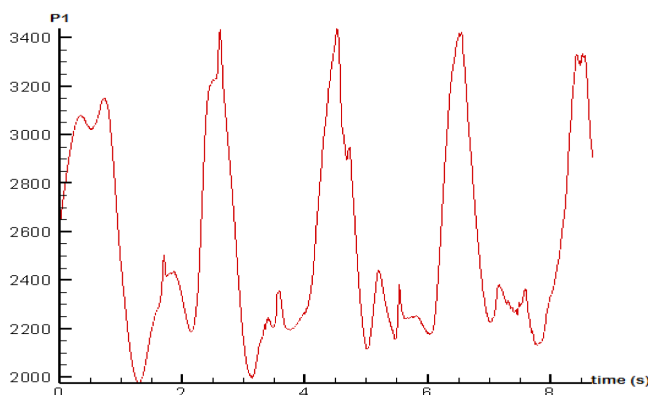

(a)

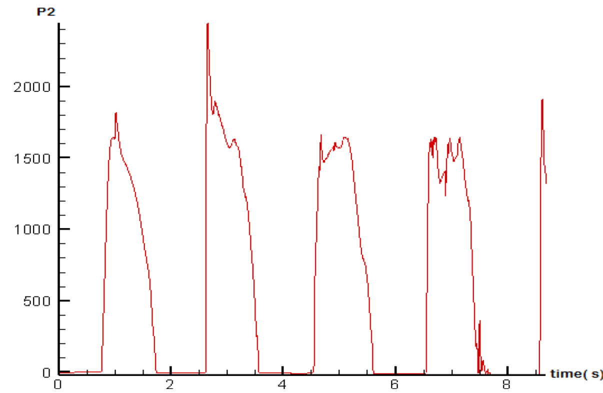

(b)

Figure 7. Pressures of water at points A and B.

3.2. Tank with one bulkhead

Figures 8 show the snapshots of our simulations. It is noticed that the amplitude of sloshing of water inside the tank is reduced considerably. The period of the oscillations is greater than that of the excitation of the tank, so there is not any resonance phenomena. From Figure 9, we can notice that the period of sloshing is almost $T = 5\,\text{s}$ greater than $T = 2\,\text{s}$.

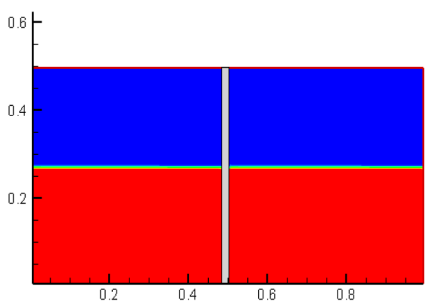

$T = 0\,\text{s}.$

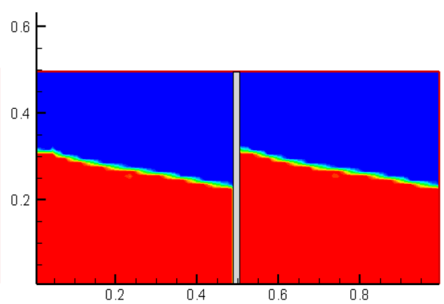

$T = 0.26\,\text{s}.$

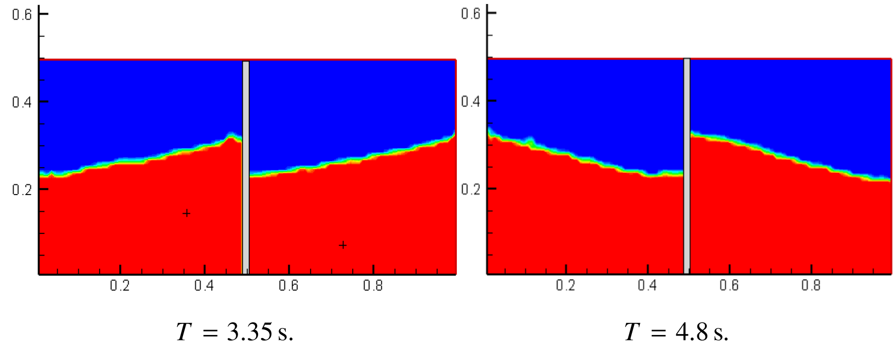

Figure 8. Sloshing in tank with one bulkhead.

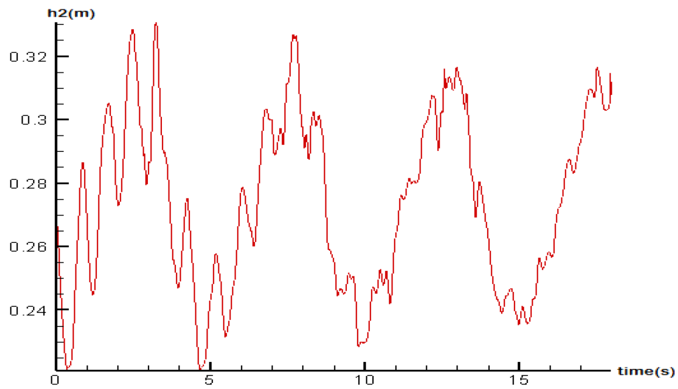

Figure 9. Height of water in tank with one bulkhead.

The pressures (in Pascal) at points A $(x = 0.5,\ y = 0.05)$ and B $(x = 1,\ y = 0.265)$ are shown in Figure 10. The period of pressure oscillations is near $T = 5$ s. Point A is bottom, the pressure is larger because of additional hydrostatic pressure. Point B is on initial free surface, where atmospheric pressure is assumed to null. Hence when the point B is in air region the pressure becomes zero and when it is in water the pressure increases until 500 Pa.

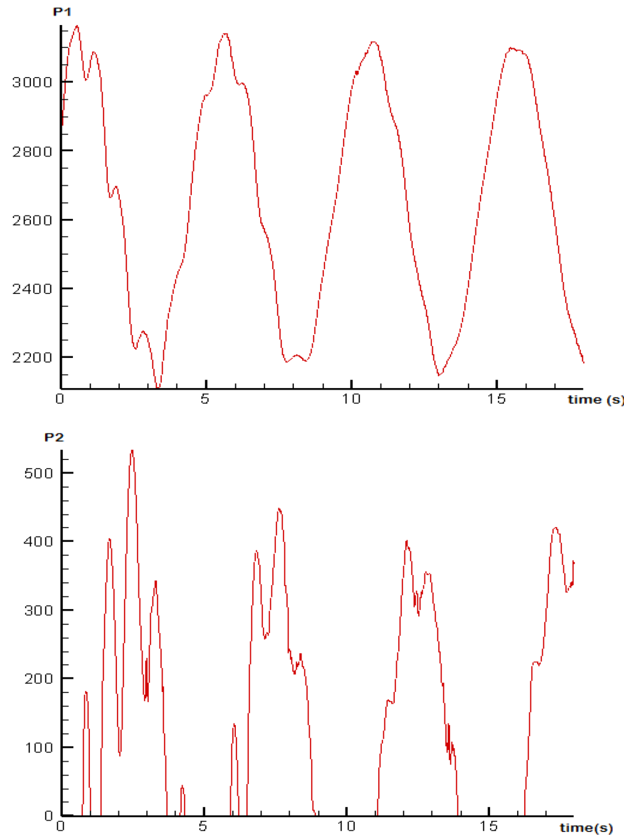

Figure 10. Pressures of water at points *A* and *B*.

4. Conclusion

In this paper, we have studied the effect of a bulkhead on liquid sloshing in a two dimensional rectangular tank using an algebraic technique of Volume of Fluid method. The numerical results show that the baffle may be considered as a damper of liquid sloshing in a tank. Indeed, it prevents the increase of the amplitude of the sloshing which can preserve the ship stability. We hope in the future that the next study will be devoted to more baffles than one in three-dimension flow.

References

[1] K. J. Rawson and E. C. Tupper, Basic Ship Theory, Hydrostatics and Strength, Vol. 1, 2001.

[2] P. Bouguer, Traité du Navire, de sa Construction et de ses mouvements, pp. 682.

[3] P. Krata, The impact of sloshing liquids on ship stability for various dimensions of partly filled tanks, Int. J. Marine Navigation and Safety of Sea Transportation 7(4) (2013).

[4] S. Colin Moore, The Principles of Naval Architecture Series, Intact Stability, 2010.

[5] A. B. Brian, Ship Hydrostatics and Stability, First published 2003.

[6] C. B. Barras and D. R. Derrett, Ship Stability for Masters and Mates, 5th ed., 2001.

[7] Y. G. Chen, K. Djidjeli and W. G. Price, Numerical simulation of liquid sloshing phenomena in partially filled containers, Computers & Fluids 38 (2009), 830-842.

[8] Hung-Pin Chien, Chun-Chung Chang and Yen-Jen Chen, Simulation of a ship with partially filled tanks rolling in waves by applying moving particle semi-implicit method, International Conference on Engineering Education, ICEE 2007.

[9] Tomasz Waclawczyk and Tadeusz Koronowiccz, Comparison of CICSAM and HRIC high-resolution schemes for interface capturing, J. Theor. Appl. Mech. 46(2) (2008), 325-345.

[10] N. Coulibaly, A. Hage and J. J. Marchal, Coupling of implicit-explicit methods for two-phase flow with a fully volume preserving method, Inter. Conference on Marine Research and Transportation, 2007.

[11] N. Coulibaly, M. Dosso and E. Danho, Numerical simulation of sloshing problem in rectangular tank, Adv. Appl. Mech. Eng. Tech. 5(1) (2014), 1-26.

[12] M. Hinatsu, Y. Tsukada, R. Fukusawa and Y. Tanaka, Experiments of two-phase flows for the joint research, Proceedings of SRI-TUHH mini-workshop on Numerical Simulation of Two-Phase Flows, National Maritime Research Institute Tokyo, Japan.

[13] J. Brackbill, D. Kothe and C. Zemach, A continuum method for modelling surface tension, J. Comput. Phys. 100 (1992), 335-354.

[14] V. Armenio, An improved MAC method (SIMAC) for unsteady high-Reynolds free surface flows, Int. J. Numer. Methods Fluids 24 (1997), 185-214.

[15] T. J. Chung, Computational Fluid Dynamics, University of Alabama in Huntsville, 2002.

[16] H. K Versteeg and W. Malalasekera, An Introduction to Computational Fluid Dynamics, The Finite Volume Method, 1995.

[17] C. Pozrikidis, Fluid Dynamics, Theory, Computation and Numerical Simulation,

University of California, San Diego, 2001.

[18] J. N. Newmann, Linearized wave resistance theory, International Seminar on Wave Resistance, Japan, 1976.

[19] C. W. Dawson, A practical computer method for solving ship-wave problems, 2nd International Conference on Numerical Ship Hydrodynamics, Berkeley, USA, 1977.

[20] G. Delhommeau, Wave Resistance Code REVA, PhD Thesis 1993, Ecole Centrale Nantes, France.

[21] Harlow and Welch, Numerical Calculation of Time Dependent Viscous Incompressible Flows of Liquid with Free Surface, Phys. Fluids 8(12) (1965), 2128.

[22] S. Osher and J. A. Sethian, Fronts propagating with curvature dependent speed: algorithms based on Hamilton-Jacobi formulation. J. Comput. Phys. 79 (1988), 12-49.

[23] DeBar, Fundamentals of KRAKEN code, Technical Report UCIR-760, LLNL, 1974.

[24] W. F. Noh and P. Woodward, SLIC (Simple Line Interface Calculation), Lecture Notes Physics, Vol. 59, Springer, New York, 1976, pp. 330-340.

[25] J. D. Ramshaw and J. A. Trapp, A numerical technique for low-speed homogeneous two-phase flows with sharp interface, J. Comput. Phys. 21 (1976).

[26] C. S. Peskin, Numerical analysis of blood flow in the heart, J. Comput. Phys. 25 (1977), 220-252.

[27] C. W. Hirt and B. D. Nichols, Volume of fluid (VOF) method for the dynamics of free boundaries, J. Comput. Phys. 39 (1981), 201-225.

[28] D. B. Kothe and W. J. Rider, Reconstructing volume tracking, J. Comput. Phys. 141(1998), 112-152; U. S department of Energy by Los Alamos National Laboratory.

[29] D. B. Kothe, W. J. Rider, S. J. Mosso and J. S. Brock, Volume Tracking of Interfaces having Surface Tension in Two and Three Dimensions, AIAA 96, no. 0859.

[30] D. Gueyffier, A. Nadim, J. Li, R. Scardovelli and S. Zaleski, Volume of fluid interface tracking with smoothed surface stress methods for three dimensional flows, J. Comput. Phys. 152 (1999), 423-456.

[31] J. Li, Calcul d'Interface Affine par Morceaux (Piecewise Linear Interface calculation), C. R. Acad. Sci. Paris, série IIb, Paris 320 (1995), 391-396.

[32] E. Aulisa, S. Manservisi and R. Scardovelli, A mixed markers and volume-of-fluid method for the reconstruction and advection of interfaces in two-phase and free boundary flows, J. Comput. Phys. 188(2) (2003), 611-639.

[33] D. B. Kothe and W. J. Rider, Comments on Modelling Interfacial Flows with Volume of Fluid Methods, Technical Report, LA-UR-3384, Los Alamos National Laboratory, www://c3.lanl.gov/~wjr/pubs.

[34] P. Sames, T. Schellin, S. Muzaferija and M. Peric, Application of two-fluid finite volume method to ship slamming, Proc. OMAE'98, Lisbon, 1998.

[35] Jeroen Gerrits, Dynamics of liquid-filled spacecraft, Numerical simulation of coupled solid-liquid dynamics, Thesis.

[36] O. M. Faltinsen and A. N. Timokha, Natural sloshing frequencies and modes in a rectangular tank with a slat-type screen, J. Sound and Vibration 330 (2011), 1490-1503.

[37] A. Bouabidi, D. Zied and M. S. Abid, Vertical baffles height effect on liquid sloshing in an accelerating rectangular tank, Int. J. Mechanics and Applications 3(5) (2013), 105-116.

[38] Murray Rudman, Volume-tracking methods for interfacial flow calculations, Int. J. Numerical Methods in Fluids 24 (1997), 671-691.

[39] Meng Huang, Bin Chen and Lilong Wu, A SLIC based on unstructured grid, J. Microgravity Science and Technology 22(3) (2010), 305-314.

[40] T. Hayase, J. A. C. Humphrey and R. Greif, A consistently formulated QUICK scheme for fast and stable convergence using finite-volume iterative calculation procedures, J. Comput. Phys. 98(1) (1992), 108-118.

[41] Wen Zhong Shen, Jess A. Michlsen and J. N. Sorensen, Improved Rhie-Chow interpolation for unsteady flow computations, AIAA Journal 39(12) (2001), 2406-2409.

[42] H. C Yee, Construction of explicit and implicit symmetric TVD schemes and their applications, J. Comput. Phys. 68 (1987), 151-179.

[43] John Thuburn, TVD schemes, positive schemes, and the universal limiter, Monthly Weather Review, Vol. 125, December 1996.

[44] S. R. Chakravarty and S. Osher, High resolution application of the Osher upwind scheme for the Euler equation, AIAA paper 83-1943.

[45] R. I. Issa and M. H. Javareshkian, Pressure based compressible calculation method utilizing total variation diminishing scheme, AIAA Journal 36(9) 1652-1657.

[46] B. P. Leonard, The ULTIMATE conservative difference scheme applied to unsteady one-dimension advection, Comput. Meth. Appl. Mech. and Eng. 88 (1991), 17-74.

[47] P. H. Gaskell, A. K. C. Lau, Curvature compensated convective transport: SMART, a new boundedness preserving transport algorithm, Int. J. Num. Meth. Fluids 8 (1988), 617-641.

[48] J. Zhu and W. Rodi, A low dispersion and bounded convection scheme, Comput. Meth. Appl. Mech. & Eng. 92 (1991), 87-96.

[49] M. S. Darwish, A New High Resolution Scheme based on the Normalized Variable Formulation 1993.

[50] O. Ubbink and R. I. Issa, Method for capturing sharp fluid interfaces on arbitrary meshes, J. Comput. Phys. 153 (1999), 26-50.

[51] Tomasz Waclawczyk and Tadeusz Koronowiccz, Modeling of the wave breaking with CICSAM and HRIC high-resolution schemes, European Conference on Computational Fluids Dynamics, ECCOMAS, CFD 2006.